Al-Mukhtar Journal of Engineering Research 07 (1): 20-28, 2023
Doi: https://doi.org/10.54172/wadd2q70

Research Article **Open Access**

Development of Drag Coefficient Correlations for Circular Cylinder Using Turingbot Symbolic Regression Software

Husam A. Elghannay[(1)], and Yousef M. F. El Hasadi[(2)]

***Corresponding author:** E-mail addresses: example@example.com Department of Mechanical Engineering, University of Benghazi, Benghazi, Libya.

Second Author: E-mail addresses: example@example.com Frederik Hendrikstraat 2628 SX, Delft, the Netherlands

Received:
12 July 2023

Accepted:
26 November 2023

Publish online:
31 December 2023

Abstract

The current paper provides a symbolic regression-based correlation for the drag coefficient for circular cylinder. The correlation is intended to be applicable over a wide range of flow regimes namely that range from the creeping flow regime up to the turbulent flow regime. Demo version of TuringBot symbolic regression software was used to develop different correlations using different sets of data. Experimental set of data was used in one run whereas steady numerical results for Reynolds number up to ~ 25 were used in generating a second set of formulas. In a different run data generated using Sucker and Brauwer (Wärme-und Stoffübertragung, 1975. 8: p. 149-158) correlation with uniform distribution in each order of magnitude was used to obtain a different set of correlations. The data was generated across five orders of magnitude of change of Re. Among all suggested formulas in the three cases, four correlations are considered for their simplicity and accuracy. The predictions of the correlations ranged from reasonably good to very good as compared to existing data and correlations. The relative error of the four developed correlations ranged between 9% and 16% when compared to experimental data for Reynolds numbers ranging from 1-10^5. In particular, one correlation was able to capture all the qualitative and quantitative changes in the drag coefficient over the different flow regimes for $0.15 < Re < 10^5$. The relative error of this correlation was comparable to Sucker and Brauwer correlation.

Keywords: Drag Coefficient; Circular Cylinder; Correlation; Machine Learning; Symbolic Regression

INTRODUCTION

The flow over fully or partially submerged bluff bodies in a fluid flow has been of interest to a vast number of researchers for several decades ago. Early documented interests of the subject may date back to da Vinci (1513) whom sketched the flow patterns around a partially submerged columns [1]. First photographs of alternating vortices past a cylinder are those reported by Henri Bénard [2], a phenomenon that is known later by Kármán-Bénard Vortex Street. Besides investigating the flow patterns around submerged bodies, the resistance force (or drag force) felt by the objects as they move through the fluid is in the core of interests of researchers. The drag force and its behavior is crucial in the design of aerofoils, automobile bodies, buildings, and airspace shuttles. To allow for a comparison of different bodies at the same flow conditions, the drag force is typically non-

dimensionaized with respect to the kinetic energy of the incoming fluid resulting in the drag coefficient (C_D).

A fundamental case of interest is the case of a circular cylinder perpendicular to a steady stream. The flow pattern generated by the flow over the cylinder exhibits a rich mosaic of flow morphologies. The drag coefficient depends on how well the air flow around the object and leaves it. Streamlined shapes and small area shapes in the flow direction generally give lower values of the drag coefficient [3]. The flow disturbance caused by the cylinder is restricted to trailing wake downstream and significantly affects the drag force. The presence of alternating shedding from the cylinder produces an oscillatory lift force on the cylinder perpendicular to the stream motion[4]. The behavior of the flow around the cylinder changes dramatically with the change of Reynolds number (Re) and so does the drag force. Two different mechanisms contribute to the drag force, the skin friction and the form drag (or pressure drag). While the first (skin friction) is directly related to shear stresses on the surface of the surface, the second is a result of the pressure difference in the direction of the drag force [3, 5].

The variation of C_D with Reynolds number is shown in Figure 1 for circular cylinder across a range of Re from 10^{-1} to 10^7. The quantitative changes of the drag coefficients over this wide range of Reynolds number are associated with tremendous variations in the qualitative flow field aspects [5]. A thorough discussion of the different flow regimes can be found in [3, 6-8]. A brief review of the different regimes is provided here for reference with Figure (1) to facilitate associating the qualitative changes in C_D with physics of the problem. For very low values of Re, say, $Re < 4$, the flow is attached to the cylinder and the streamlines are almost symmetrical and come together as they pass over the cylinder. This is a direct result of high viscosity which dominates fluid inertia effects. This viscous flow regime is called Stokes flow. As Re is increased for up to 40, separation occurs on the aft of the cylinder forming two stable distinct vortices which are stationary in their place. The vortices become unstable beyond this limit and start alternate regular shedding at the wake region (called Karaman vortex street). Further increase in Re causes the Karman vortex street to turn into turbulent and later changes into a distinct wake ($150 < Re < 300$). The separation point of the boundary layer shifts towards the back of the cylinder along the surface with the transition to fully turbulent flow.

The drag coefficient remains at an almost constant value of about one at the range of $10^3 < Re < 3\times10^5$. Further increase in Re ($3\times10^5 < Re < 3\times10^6$) makes the flow in the outer region of the boundary layer to changes to turbulent flow causing reattachment followed by another separation of the boundary layer at the back face of the cylinder. As the flow changes to turbulent the wake thickness shrinks resulting in a reduction in the pressure drag on the cylinder to undergo a dramatic drop around $Re = 3\times10^5$ (also known as the drag crises). Beyond $Re > 3\times10^6$, a direct transition of the boundary layer to turbulent flow takes place at some point on the forward face. The separation of boundary layer at this case is estimated at an angular location slightly less than 120^o on the back surface. The separation points on the back surface shifts closer to the top and bottom of the cylinder, producing a thicker wake, thus larger pressure drag.

Three distinct flow regimes can be used to characterize the variations of the drag coefficient of the cylinder known as subcritical, supercritical and transcritical based on their location from the critical Re at which the drag crisis takes place. The roughness of the cylinder surface affects both the value of Re at which the drag crisis takes place and the value of the drag coefficient after the drag crisis. More details and investigations about the drag crisis can be found in [6, 10].

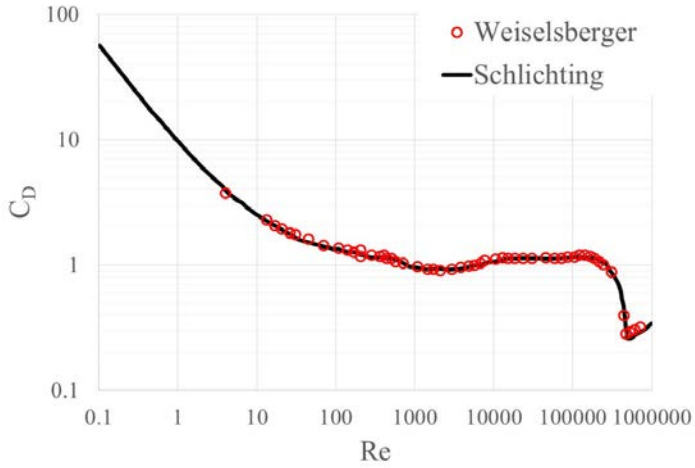

Fig. 1: Drag vs. Reynolds number for infinitely long circular cylinder (reproduced from [9]). Void circles are experiments made by Wieselsberger, the solid line is advised by Schlichting.

Qualitatively speaking the regimes and general shape of the C_D vs Re plot of flow over circular cylinder is similar to that of flow over a sphere. However, much more research is dedicated towards formulating a drag correlations for spherical particles compared to those for cylinders. Particles, bubbles, and droplets which are found in vast industrial and environmental systems can be reasonably approximated as spherical particles and hence come the significance of investigating spheres over cylinders. As a result the literature is saturated of correlations for drag over spheres which is yet worth further investigation. Symbolic regression was used to develop correlations of the drag over sphere by Baratti et al. [11] and El-Hasadi & Padding [12] using large volume of experimental data. Development of drag formula for spheroids and spherocylinder particles using limited size of high fidelity data using symbolic regression was also performed by El-Hasadi & Padding [13]. To the best of the authors' knowledge, no such use is reported to develop a correlation pertaining the drag over cylinder. The size of data used in the current work is not sizeable, but with no much notable variability.

A thorough review of all the existing correlations and experimental data is beyond the scope of this work and can be found in [9, 14, 15]. Selected correlations which includes the most commonly used in relevant literature are first outlined in the next section and their agreement with most common experimental data is reviewed. The software used in the current work is presented in section and selected correlations obtained by the software are presented in section 3. A discussion of the performance and limitations of the found formulas is provided in section 3 as well.

1. METHODOLOGY

1.1 Review of existing data and correlations

Stokes pioneered investigating the flow over spheres and cylinder at very low Re (also called creeping flow regime Re <<1). Stokes analytically solved the steady drag over a sphere in infinite medium but stated that no solution exists in flow over cylinders [16]. His postulate triggered a researchers to perform theoretical and experimental studies with varying qualitative and quantitative agreement [17]. The unclearness of the data is not well defined in many cases leading to conflicting sets of data that requires careful reevaluation and attempts to correct [18].

One of the most commonly used correlations is that of Kaplun [19] whom used matched asymptotic expansion to improve the approximate solution provided by lamb [20] to Stokes paradox

$$C_D = \frac{8\pi}{Re}\left[\left(ln\left(\frac{7.406}{Re}\right)\right)^{-1} - 0.87\left(ln\left(\frac{7.406}{Re}\right)\right)^{2}\right] \quad (1)$$

Reynolds number herein is based on the diameter of the cylinder. The formula diverges for Re values >1. White [14] offered a simple curve-fit formula which is reasonable agreement up to the drag crisis (Re < 250000). The data used in generating the correlation are from Tritton [21] and Wieselesberger [22]

$$C_D = 1 + \frac{10}{Re^{2/3}} \quad (2)$$

A roughly derived formula is suggested by Munson et al. [3] in which separation of the boundary layer is assumed to take place at 109° (measured from stagnation point).

$$C_D = 1.17 + \frac{5.93}{\sqrt{Re}} \quad (3)$$

The first term on the RHS comes from form drag while the second represents skin friction. The skin friction term was assumed to have similar dependencies between C_D and Re as that of a flat plate.

An accurate curve-fit formula [14] was proposed by Sucker & Brauwer [23]

$$C_D = 1.18 + \frac{6.8}{Re^{0.89}} + \frac{1.96}{\sqrt{Re}} - \frac{0.0004Re}{1 + 3.63 \times 10^{-7}Re^2} \quad (4)$$

Mapping of the above correlations on C_D vs. Re diagram that contains a compilation of existing data as made by Panton [7] is provided in Figure (2). The steady numerical (blue dashed line) results line is for steady numerical results by Hamielec and Raal (1969) [24] and Fornberg [25] assuming steady flow. Kaplun correlation (Eq. (1)) diverges for Re >1 while Munson's correlation (Eq. (2)) may be applied to up to Re ~ 3×10^5. Munson's formula shows reasonable agreement for $2 > Re > 10^4$ but shows a different "slope" when plotted on a log-log scale of the C_D vs. Re plot. Although predictions of White's formula (Eq. (2)) is superior to that of Munson's, it fails to capture the minimum C_D value at $10^3 < Re < 10^4$. Sucker and Brauwer's formula (Eq. (4)) outperforms all the presented correlations and captures almost all qualitative behaviors before the drag crisis.

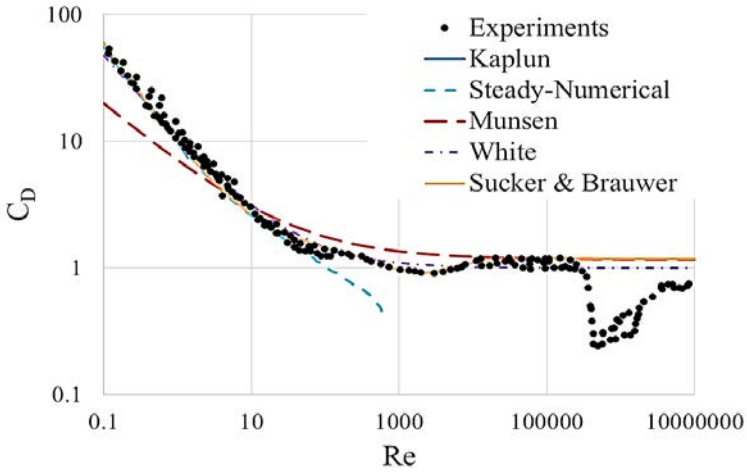

Fig. 2: Comparison of different correlations with experimental data for drag over circular cylinder. Experimental data compiled by Panton [7]**.**

1.2 Analysis Software

TuringBot symbolic regression software is chosen to perform the regression task. The free Demo version, however, has a limitation on both the number of data points and the number of inde-

pendent variables. The maximum number of data points is 50 whereas a variable can only be a function of other two parameters. Once the data is loaded, the target parameter along with the ratio of test/train sets is selected before running the job. It is optional to shuffle the data before running the job. Although the software defaults the parameter used to evaluate the accuracy to the root mean square (*rms*) value of the target variable, it is possible to select different criterion from a dropdown list. Once the task is executed, the software suggests a list of possible fitting functions (starting from a bare average). The software keeps refining (or replacing) the proposed formulas producing more accurate fits until the user decides to halt it. TuringBot interface allows for visualization of the different suggested solutions and how they fit the original data. Since the current work assumes $C_D=f(Re)$, the Demo version is appropriate given that the used data does not include much uncertainty.

2. RESULTS AND DISCUSSIONS

Selected sets of data were used to generate a drag formula and led to the following formulas:

$$C_D = \left(9.29 - shin^{-1}(3.19 - 0.000545Re)\right)/shin^{-1}(Re) \quad (5)$$

$$C_D = 1.268 + \frac{8.39}{Re^{0.82}} \quad (6)$$

$$C_D = 1.074 + \frac{8.76}{Re^{0.743}} \quad (7)$$

$$C_D = 1.154 + \frac{8.02 - 4.657 \times 10^{-5} Re^2}{(Re - 0.119)^{0.7229} + 6.601 \times 10^{-5} Re} \quad (8)$$

Data from Wieselsberger [22] at Re ranges from ~ 4 -105000 was used to generate Eq. (5) thus excluding the drag crisis experimental data. The data is a subset of the data in Figure 2 and is displayed in Figure 1. Although hyperbolic functions are not commonly used in drag formulas, Barati's correlation [11] for drag over sphere is rich of trigonometric and hyperbolic functions. It is not clear to us at the time being if these functions can actually be linked to the physics of the problem or they exist because of their ability to fit complicated behavior. The steady numerical results of Hamieleec & Raal [24] and Fornberg [25] are found to be in very good agreement with the average experimental data trend line advised by Schlichting (see Figure (1)) until Re ~25 [9]. Beyond Re ~25 deviations between the steady simulations and the experiment take place possibly because unsteadiness is initiated in the form of vortex shedding. The line at which the steady results almost match the experimental results was digitized to ~ 50 data points ($0.24 < Re < 24$) which were fed to TuringBot to generate Eq. (6). The third data set was generated using Sucker and Brauwer's correlation (Eq. (4)) for ($0.1 < Re < 10^5$) with equal number of data points in each order of magnitude. In the first two runs 75/25 test/train ratio was selected, however, all the data was used in the training (no testing) when Eqs. (7 & 8) were obtained. The former strategy of not spending part of the data in testing the trained model was adapted to ensure having equal weights for the different regimes in generating the correlation.

Comparison of Eqs. (5 - 8) is shown in the Figure (3). Eq. (5) shows some deviation at very low Reynolds number most likely because of the uncertainty in the data point used at Re~4 which affected the extrapolation process at lower Reynolds number values. On the other hand Eq. (6) shows quite good agreement for flow regimes before the drag crisis. Similar to the correlation by White (Eq. (2)), the physics embedded in the minimum Re at $10^3 < Re < 10^4$ are, however, not captured. Due to the relatively low number of data points at this region, it would be hard for the algorithm to capture the trend in this regime. Such drawback is avoided in the third set of data in which the data is generated in similar distribution at each "decade". Eq. (7) has similar structure to Eq. (6) which

comes from steady data but better agreement with experimental data at high Reynolds number. Both correlations converge to a constant value of C_D at high Re values ($Re > 10^3$). As can be seen from the equation itself, Eq. (7) converges to a value of 1.074 which is very close to the suggested value of one by White (Eq. 6). This Reynolds number-free term can be linked to the form drag as outlined by Munson et al. [3] and the value to which it converged could be linked to the separation angle of the boundary layer. The separation angle as a function of Re is a subject of interest to many researchers (e.g.[26, 27]).

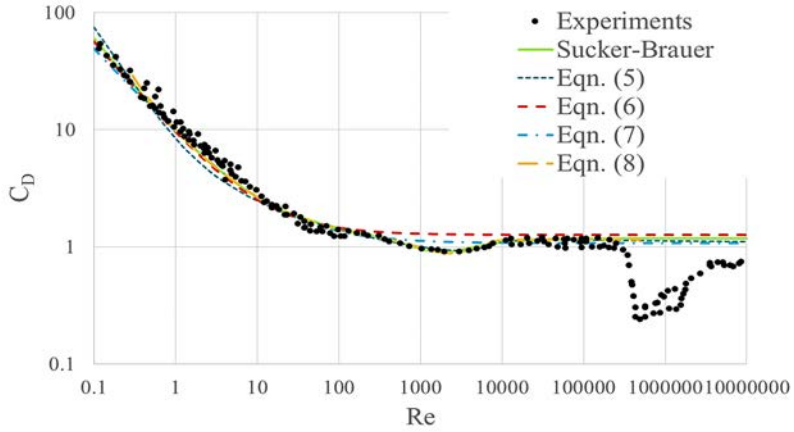

Figure 3. Comparison of the current results with available experimental data and empirical correlation of Sucker and Brauwer [23]

Table (1) lists the *rms* error for the proposed equations against the data used in testing, and the average relative error from the data of Wieslesbrger and finally against the available experimental data at Re ranges from ~1-10^5. All suggested correlations have low average rms error in their training data. When compared to Wielesberger experimental data which is used to generate Eq. (5) the relative error was the least for Eq. (5), however, Eq. (8) show comparable performance. Although Eq. (6) shows the highest deviations of ~16%, its deviation is not bad provided that it was generated using steady results for up to Re ~24. When the experimental data over a wide range is considered, Eq. (7) become comparable to both Eqs. (8) and Sucker and Brauwer (Eq. (4)). The relatively large error is mainly because of the variations of the results of the experimental data itself. The inability of Eq. (7) to capture the behavior at $10^3 < Re < 10^4$ is alleviated as a consequence of the limited number of data at that regime as compared to the total number of data points used. The performance of Eq. (5) now deteriorated as it diverges outside its training data regime. Indeed Eq. (8) has the best agreement among all obtained correlation over the wide range of Re. The local minimum is captured and the agreement with Sucker-Bauwer's correlation is obvious. Interestingly the correlation has consistently shown somewhat lower relative error when compared to the experimental data. The correlation, however, diverges beyond Re values lower than ~0.12 possibly because of the existence of negative number (at the denominator) raised to a negative number.

Table (1). Comparison of relative average error of proposed correlations with experimental data

Formula	Average rms error in training data	Average relative error %	
		Wieselsbrger	All Available
Eq. (5)	0.0477752	2.37	13.26
Eq. (6)	0.0728236	15.9	16.07
Eq. (7)	0.088027	6.3	9.83
Eq. (8)	0.0237282	2.89	9.15
S&B	NA	3.14	9.51

A close view of the performance of different correlations at low Re values is provided in Figure (4) for 0.1< Re < 10. It can be seen that White's correlation has the best agreement with experimental data at for 1 < Re <10. The correlation however underpredicts the experiments at lower values of Re and may depart at further low values. Equation (8) is in very good agreement with Sucker and Brauwer's formula and the steady numerical results.

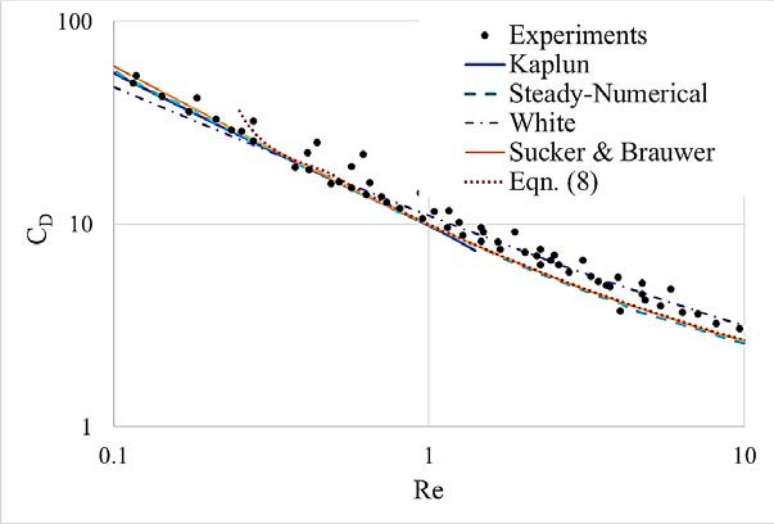

Fig. 4: Comparison of best correlations with experimental data at low Re values

3. Conclusions and Recommendations for Further Work

Symbolic regression was successfully used to generate a correlation that predict the drag coefficient for a wide range of Reynolds number. Although the developed correlation captured all the qualitative changes in C_D in the different flow regimes it does not extrapolate beyond the training regime used. In fact none of the existing correlations as of yet was capable of predicting the behavior at the drag crisis. The obtained correlation was developed by generating a reasonably small set of data from reliable correlation. The former strategy was adapted by El-Hasadi and Padding [12] in investigating the existence of logarithmic terms in the drag over sphere and is the best recommended in the absence of highly accurate measurements that covers the whole regime. Further investigation is required in the creeping flow regime if Stokes paradox is to be tackled using symbolic regression. Investigation of the existence of logarithmic terms and whether it is possible to predict the drag crisis in a generic formula are other research extensions that would be carried out using symbolic regression. For the former purpose, larger volume of data may be required.

REFERENCES

[1] Forouzi Feshalami, B., S. He, F. Scarano, L. Gan, and C. Morton, A review of experiments on stationary bluff body wakes. Physics of Fluids, 2022. 34(1): p. 011301.

[2] Bénard, H., Formation des centres de giration à l'arrière d'un obstacle en mouvement. Compt. rend., 1908. 147: p. 839.

[3] Munson, B.R., D.F. Young, and T.H. Okiishi, Fundamentals of fluid mechanics. Oceanographic Literature Review, 1995. 10(42): p. 831.

[4] Pritchard, P.J. and J.W. Mitchell, Fox and McDonald's introduction to fluid mechanics. 2016: John Wiley & Sons.

[5] Thom, A., The boundary layer of the front portion of a cylinder. 1928, HM Stationery Office.

[6] Anderson, J., EBOOK: Fundamentals of Aerodynamics (SI units). 2011: McGraw hill.

[7] Panton, R.L., Incompressible flow. 2013: John Wiley & Sons.

[8] Markland, E., A first course in air flow. 1976: Tecquipment limited.

[9] Schlichting, H. and J. Kestin, Boundary layer theory. Vol. 121. 1961: Springer.

[10] Kreith, F., Fluid mechanics. 1999: CRC press.

[11] Barati, R., S.A.A.S. Neyshabouri, and G. Ahmadi, Development of empirical models with high accuracy for estimation of drag coefficient of flow around a smooth sphere: An evolutionary approach. Powder Technology, 2014. 257: p. 11-19.

[12] El Hasadi, Y.M. and J.T. Padding, Do logarithmic terms exist in the drag coefficient of a single sphere at high Reynolds numbers? Chemical Engineering Science, 2023. 265: p. 118195.

[13] El Hasadi, Y.M. and J.T. Padding, Solving fluid flow problems using semi-supervised symbolic regression on sparse data. AIP Advances, 2019. 9(11): p. 115218.

[14] White, F.M. and J. Majdalani, Viscous fluid flow. Vol. 3. 2006: McGraw-Hill New York.

[15] Niemann, H.-J. and N. Hölscher, A review of recent experiments on the flow past circular cylinders. Journal of Wind Engineering and Industrial Aerodynamics, 1990. 33(1-2): p. 197-209.

[16] Stokes, G.G., On the effect of the internal friction of fluids on the motion of pendulums. 1851.

[17] Khalili, A. and B. Liu, Stokes' paradox: creeping flow past a two-dimensional cylinder in an infinite domain. Journal of Fluid Mechanics, 2017. 817: p. 374-387.

[18] Lienhard, J.H., Synopsis of lift, drag, and vortex frequency data for rigid circular cylinders. Vol. 300. 1966: Technical Extension Service, Washington State University Pullman, WA.

[19] Kaplun, S., Low Reynolds number flow past a circular cylinder. Journal of Mathematics and Mechanics, 1957: p. 595-603.

[20] Lamb, H., Hydrodynamics. 1924: University Press.

[21] Tritton, D.J., Experiments on the flow past a circular cylinder at low Reynolds numbers. Journal of Fluid Mechanics, 1959. 6(4): p. 547-567.

[22] Wieselsberger, C., New data on the laws of fluid resistance. 1922.

[23] Sucker, D. and H. Brauer, Investigation of the flow around transverse cylinders. Wärme-und Stoffübertragung, 1975. 8: p. 149-158.

[24] Hamielec, A. and J. Raal, Numerical studies of viscous flow around circular cylinders. The physics of fluids, 1969. 12(1): p. 11-17.

[25] Fornberg, B., A numerical study of steady viscous flow past a circular cylinder. Journal of Fluid Mechanics, 1980. 98(4): p. 819-855.

[26] Wu, M.-H., C.-Y. Wen, R.-H. Yen, M.-C. Weng, and A.-B. Wang, Experimental and numerical study of the separation angle for flow around a circular cylinder at low Reynolds number. Journal of Fluid Mechanics, 2004. 515: p. 233-260.

[27] Islam, T., S.R. Hassan, and M. Ali, Flow separation phenomena for steady flow over a circular cylinder at low Reynolds number. International Journal of Automotive and Mechanical Engineering, 2013. 8: p. 1406.